Published in final edited form as:
Diabetes. 2002 March ; 51(3): 797–802.

The effects of rosiglitazone on insulin sensitivity, lipolysis, and hepatic and skeletal muscle triglyceride content in patients with type 2 diabetes

Adam B. Mayerson[1], **Ripudaman S. Hundal**[1], **Sylvie Dufour**[1,3], **Vincent Lebon**[1,3], **Douglas Befroy**[1,3], **Gary W. Cline**[1], **Staffan Enocksson**[1], **Silvio E. Inzucchi**[1], **Gerald I. Shulman**[1,2,3], and **Kitt F. Petersen**[1]

[1]Department of Internal Medicine, Yale University School of Medicine New Haven, CT 06510

[2]Department of Cellular & Molecular Physiology, Yale University School of Medicine New Haven, CT 06510

[3]Department of Howard Hughes Medical Institute, Yale University School of Medicine New Haven, CT 06510

Abstract

We examined the effect of three months of rosiglitazone treatment (4mg BID) on whole body insulin sensitivity and *in vivo* peripheral adipocyte insulin sensitivity as assessed by glycerol release in microdialysis from subcutaneous fat during a two-step (20 and 120 mU/m^2-min) hyperinsulinemic-euglycemic clamp in nine type 2 diabetic subjects. In addition the effects of rosiglitazone on liver and muscle triglyceride content were assessed by ^{1}H NMR spectroscopy. Rosiglitazone treatment resulted in a 68% ($P<0.002$) and a 20% ($P<0.016$) improvement in insulin stimulated glucose metabolism during the low and high dose steps, respectively, which was associated with ~40% reductions in both plasma fatty acid concentration ($P<0.05$) and hepatic triglyceride content ($P<0.05$). These changes were associated with a 39% increase in extramyocellular lipid content ($P<0.05$) and a 52% increase in the sensitivity of peripheral adipocytes to the inhibitory effects of insulin on lipolysis ($p=0.04$).

In conclusion these results support the hypothesis that thiazolidinediones enhance insulin sensitivity in patients with type 2 diabetes by promoting increased insulin sensitivity in peripheral adipocytes, which results in lower plasma fatty acid concentrations and a redistribution of intracellular lipid from insulin responsive organs into peripheral adipocytes.

Keywords

thiazolidinediones; type 2 diabetes mellitus; lipolysis; insulin resistance; NMR

Introduction

Although thiazolidinediones (TZDs) are now widely used to treat type 2 diabetes their mechanism of action remains unknown. While it is well established that they enhance insulin sensitivity by acting as ligands for the transcription peroxisome proliferator-activated receptor-gamma (PPAR-γ) (1,2). PPAR-γ is predominantly expressed in adipose tissue,

Corresponding author: Kitt F. Petersen, M.D., Department of Internal Medicine, Yale University School of Medicine, 333 Cedar Street, Fitkin 1, Box 208020, New Haven, CT 06520-8020, Phone: (203) 737-1942, Fax: (203) 737- 2174, kitt.petersen@yale.edu.

whereas the improvement in insulin sensitivity occurs predominately in skeletal muscle (3–5) where PPAR-γ expression is relatively low (1,2). This paradox suggests that the TZDs may indeed modulate key communicating signals between fat and muscle such as leptin (6), adiponectin (7), TNF-α (8), resistin (9), and fatty acids (10–13). In support of fatty acids being an important factor in this regard recent studies have demonstrated a strong relationship between tissue lipid content and insulin resistance in both skeletal muscle (14–20) and liver (15,16,21).

In this study we examined the hypothesis that thiazolidinediones improve insulin sensitivity in patients with type 2 diabetes by promoting the redistribution of triglyceride from liver and muscle to peripheral adipocytes. In order to examine this hypothesis we analyzed the effects of rosiglitazone, a TZD, in subjects with type 2 diabetes using several different complimentary methodologies. ^{1}H NMR spectroscopy was used to assess triglyceride content in liver and muscle in conjunction with the hyperinsulinemic-euglycemic clamp and indirect calorimetry to assess insulin sensitivity. The effects of rosiglitazone on peripheral adipocyte lipolysis during the clamp was assessed by microdialysis measurements of glycerol release from subcutaneous fat.

Research Design and Methods

Subjects

Nine nonsmoking healthy subjects with type 2 diabetes participated in this study. Their clinical and metabolic profiles are detailed in Table 1. Generally, this was a middle-aged, obese, but well-controlled group of patients. At the time of enrollment, six subjects were taking either metformin, a sulfonylurea, or both, and the remaining three subjects were managing their diabetes with diet alone. Informed written consent was obtained from all subjects after the aims and potential risks of the study were explained to them. The protocol was approved by the Yale University School of Medicine Human Investigation Committee.

Study Design

After a medical screening, a “wash-out” period of 10–14 days was allowed for the discontinuation of any prior oral anti-diabetic regimen. For the three days prior to the start of the trial, subjects consumed a weight maintenance diet according to the guidelines of the American Diabetes Association (60% carbohydrate, 20% protein, 20% fat), evenly divided between three meals. Subjects were then admitted to the Yale/New Haven Hospital General Clinical Research Center (GCRC) where they underwent a series of metabolic investigations. After these baseline studies, rosiglitazone was taken orally at a dosage of 4 mg BID for 10–12 weeks. The subjects were then readmitted to the GCRC and underwent the identical metabolic investigations conducted during the baseline evaluation. During the treatment period, subjects were evaluated every two weeks to ensure compliance and to assess for adverse events, including liver function test monitoring.

Insulin Clamp Procedure—At 8:00 a.m., a 3-hour primed (corrected for ambient fasting plasma glucose level), continuous (2 mg/m^2 body surface area/minute) infusion of [6,6-^{2}H]-glucose isotope was begun through an antecubital vein. During the third hour of infusion, a retrograde cannula was inserted into a vein in the contralateral hand, which was warmed for the sampling of "arterialized" venous blood. A small volume of 0.9% NaCl flowed through the sampling cannula in order to maintain patency. Blood samples were withdrawn at 10 minute intervals during the final 40 minutes of the third hour for the measurement of plasma glucose and insulin levels, and glucose isotope enrichment. After 3 hours of isotope infusion, a two-step hyperinsulinemic euglycemic clamp was initiated, as previously described (3). During the first step (low dose) insulin was infused at 20 mU/m^2-min for 120

minutes to assess insulin's effects on peripheral adipocyte lipolysis. During the second step (high dose) insulin was infused at 120 mU/m^2-min for 240 minutes to assess insulin's effects on peripheral glucose disposal and suppression of endogenous glucose production.

Indirect calorimetry—During the final 30 minutes of the basal infusion, and each step of the insulin clamp, indirect calorimetry using the ventilated hood technique (Deltatrack Metabolic Monitor, Sensorimedics, Anaheim, CA) was performed to measure basal fasting rates of glucose and lipid oxidation, as previously described (22).

Adipose tissue microdialysis—The microdialysis probe (CMA/60, CMA, Microdialysis, Solna, Sweden) and details of the microdialysis experiments have been previously described (23,24). Briefly, a dialysis tubing (20 mm shaft, 30 mm membrane 20 kD) is attached to the end of double lumen polyurethane tubing. The perfusate enters through the outer lumen, flows to the microdialysis membrane, and is subsequently collected (dialysate) throughout the outer lumen. Once steady state is reached, the composition of the dialysate reflects that of the interstitial fluid (25). After an overnight fast, and before the baseline infusions were begun for the insulin clamp, two dialysis probes were inserted percutaneously into the subcutaneous tissue of the abdomen, 4–6cm lateral to the umbilicus. To estimate regional adipose tissue blood flow, a microdialysis ethanol technique was used as previously described and validated (26,27). Briefly an ethanol-based perfusate (50 mmol/ liter) was infused through each probe using a microinjection pump (CMA/106 for a perfusate rate of 0.3 μliters/min) and a Harvard pump (2 microliters/ minute). After an initial 30 minute "wash-out" period, dialysate samples were collected every 30 minutes for the entire 9-hour time period (3 hour baseline and 6 hour two-step clamp).

^{1}H-NMR spectroscopy of hepatic and intramuscular triglyceride content—At 7 AM on the morning following the insulin clamp, and after a 12 hour fast, subjects were transported by wheelchair to the Yale Magnetic Resonance Center. Localized ^{1}H-NMR spectra of the soleus muscle were acquired on a 2.1T Biospec system (Bruker Instruments Inc., Billerica, MA), using a coil assembly consisting of two circular hydrogen-1 coil loops (13 cm diameter each), arranged spatially to generate a quadrature field. During the measurements, the subject remained supine, and the gastrocnemius-soleus complex of the right leg was positioned within the homogeneous volume of the magnet. Scout images were acquired in order to position the volume of interest. Volumes of interest (15mm × 15mm × 25mm) were centered within the soleus muscle, positioned to avoid vascular structures and gross adipose tissue deposits. Localized shimming in the soleus was performed using FASTERMAP (28) with typical line widths of ~10 Hz obtained. Localized proton spectra were then collected using a PRESS sequence with the following parameters: repetition time (T_R) = 3s; echo time (T_E) = 21.1ms; 8192 data points over 5000 Hz spectral width; 128 scans. Signals in the time domain were multiplied by a Gaussian function prior to Fourier transformation and manual phase correction. ^{1}H resonances were assigned to water and methyl/methylene of triglycerides from their chemical shift, in agreement with Schick et al. (29), and were line fitted using the Mac-Nuts-PPC software package (Acorn NMR, Inc., CA, USA). Intramyocellular lipid (triglyceride) content (IMCL) and extramyocellular lipid content (EMCL) were calculated from the peak areas of intramyocellular CH_2 and extramyocellular CH_2, respectively, with respect to the water peak area, corrected for T_1 and T_2 relaxation effects. IMCL and EMCL content were then expressed as a percentage of water content.

Localized ^{1}H-NMR spectra of the liver were obtained using a 12 × 14 cm butterfly ^{1}H observation coil placed rigidly over the lateral aspect of the abdomen. Placement of the volume of interest (15mm × 15mm × 15mm) within the liver was ensured by imaging the liver with a multi-slice gradient echo sequence. Prior to each measurement, water signal was

optimized using a shimming procedure, where lipid signal (predominantly from subcutaneous fat) was suppressed using an inversion recovery method optimized to null the subcutaneous fat signal. Localized proton spectra were collected using a modified PRESS sequence with the following parameters: T_R = 3s; T_E = 24.1ms; 8192 data points over 5000 Hz spectral width; 64 scans. A saturation slice centered on the chest wall was applied to prevent contamination from subcutaneous adipose tissue. The spatial position of the saturation slice was determined for each subject from the scout image. A Lorentzian filter of 5Hz was applied before Fourier transformation and manual phase correction. Hepatic triglyceride content was calculated from the area of intrahepatic CH_2 resonance relative to the area of the water resonance, using the integration routine of Paravision software (Bruker, Billerica, MA), and then expressed as a percentage of water content.

Body composition analysis—Dual-energy x-ray absorptiometry (DEXA) scanning (Hologic QDR-4500 W, Hologic, Bedford, MA) was performed with the subject in the supine position. Fat and lean body mass in each arm, each leg, the trunk, and the head were calculated assuming 17% brain fat and lean body consisting of 73% water (30).

Analyses

Plasma glucose concentrations were measured using the glucose oxidase method with a Beckman Glucose Analyzer II (Beckman Instruments, Fullerton, CA). Plasma immunoreactive insulin concentrations were measured with a double-antibody radioimmunoassay (Diagnostic System Labs, Webster, TX). Plasma fatty acid concentrations were determined using a microfluorimetric method (31). Gas chromatography mass spectrometer analysis of enrichment of [6,6-^{2}H]-glucose in plasma and infusates was performed using the penta-acetate derivative of glucose (32). Gas-chromotography mass spectrometer analysis was performed with a Hewlett-Packard 5971A Mass Selective Detector (Wilmington, DE) operating in the positive chemical ionization mode, with methane as reagent gas. Gas chromatography conditions were isothermal at 200° C, and ions with m/z 331, 332, and 333 were monitored for glucose C1 through C6 ^{13}C atom percent enrichment.

Indirect Calorimetry—Basal and insulin-stimulated glucose and lipid oxidation rates were measured by the ventilated hood technique using a Deltatrack Metabolic Monitor (Sensorimedics, Anaheim, CA) as previously described (22).

Adipose Tissue Microdialysis—Microdialysate glycerol was measured using an enzyme linked colorimetric determination of 0.5 μl samples by a CMA 600 microdialysis analyzer. (CMA 600 Microdialysis, N. Chelmsford, MA). Ethanol concentrations were determined by a YSI analyzer (YSI, Yellow Springs, CA).

Calculations

Insulin Clamp—The rates of glucose infusion were calculated in 20-minute blocks between 80–120 minutes during the low dose insulin clamp and between 300–360 minutes of the high dose insulin clamp. The data were corrected for urinary glucose and glucose space, averaged for each step of the clamp study, and expressed as μmol glucose/m^2-min.

Clamped glucose disposal rate (GDR_c) was calculated using the following formula:

$$GDR_c = GP_c + GIR,$$

Where GP_c represents endogenous glucose production during the clamp and GIR represents the mean glucose infusion rate (mg/m^2-min) during the clamp procedure (300 to 360 minutes).

Basal glucose production (GP_b) was calculated using the following formula:

$$GP_b=(f/BSA) \times ([enrichment_{inf}/enrichment_{plasma}] - 1),$$

where f = basal [6,6-^{2}H] glucose infusion rate (mg/min), BSA = body surface area (m^2), $enrichment_{inf}$ = [6,6-^{2}H] glucose infusate enrichment (%), and $enrichment_{plasma}$ = steady-state basal plasma [6,6-^{2}H] glucose enrichment (%). (The term "enrichment" refers to the ratio of glucose isotope to naturally occurring (^{12}C) glucose, expressed as a percentage.)

Clamped glucose production (GP_c) during the second step (120 mU/m^2-min) of the hyperinsulinemic-euglycemic clamp was calculated using the following formula:

$$GP_c=GIR \times ([enrichment_{inf}/enrichment_{plasma}] - 1),$$

where GIR = mean glucose infusion rate (mg/m^2-min) during the clamp procedure (300 to 360 minutes), $enrichment_{inf}$ = exogenous [6,6-^{2}H] glucose infusate enrichment (%), and $enrichment_{plasma}$ = steady-state clamped plasma[6,6-^{2}H] glucose enrichment (%).

Indirect Calorimetry—The nonprotein respiratory quotients for 100% oxidation of fat and for oxidation of carbohydrates were 0.707 and 1.00, respectively (22). Nonoxidative glucose metabolism was calculated by subtracting the amount of glucose oxidized from the total amount of glucose infused.

Glycerol Turnover—Glycerol turnover (R_a[Glycerol]) at baseline and during the 2-steps of the insulin clamp was calculated using the following formula:

$$R_a[\text{Glycerol}]=(f/BSA) \times ([enrichment_{inf}/enrichment_{plasma}] - 1),$$

where f = basal [$^2H_5$]-glycerol infusion rate (mg/min), BSA = body surface area (m^2), $enrichment_{inf}$ = [$^2H_5$]-glycerol infusate enrichment (%), and $enrichment_{plasma}$ = steady-state basal plasma [$^2H_5$]-glycerol enrichment (%).

The percent glycerol suppression from adipocytes was calculated using the following formula:

$$\frac{Gly_b - Gly_{120'}}{Gly_b} \times 100\%$$

where Gly_b represents the serum glycerol concentration at baseline and Gly_{120}' represents that at 120 minutes of the clamp.

Adipose Blood Flow—The change in local adipose blood flow during the hyperinsulinemic-euglycemic clamp was estimated using ethanol (ETOH) recovery rates, which is expressed as a percentage using the following formula:

$$\frac{ETOH_{out}}{ETOH_{in}} \times 100\%$$

Where $ETOH_{in}$ represents the ethanol concentration measured in the perfusate, whereas $ETOH_{out}$ represents the ethanol concentration in the dialysate.

Statistical Analyses

All statistical analyses were performed using Statview® software (Abacus Concepts, Inc., Berkley, CA). All data are presented as means ± SEM. Pre- to post-therapy values are compared using a paired t-test, with significance reached by a p-value of <0.05.

Results

Table 2 shows the changes in pertinent fasting laboratory studies before and after therapy. After 3 months of rosiglitazone, mean fasting plasma glucose concentrations decreased by 12.2 ± 3.7% (p= 0.02), mean insulin concentrations decreased by 23.7 ± 6.9% (p=0.03), while mean fasting plasma fatty acid concentrations decreased by 38.8 ± 4.6% (p= 0.003). While there were no significant changes in serum hepatic transaminase levels, both alkaline phosphatase (−15.7 ± 3.8 %, p=0.007) and γglutaryltranspeptidase (−38.8 ± 4.6%, p=0.001) were significantly reduced by rosiglitazone therapy. No appreciable change in HbA1c was detected, since the baseline value reflected the degree of glycemic control achieved with the subjects' prior antidiabetic regimen.

Clamp Results

Glucose Metabolism—Insulin levels were similar during both steps of the insulin clamp before and after treatment (Figure 1). During the low-dose clamps, the mean insulin-stimulated rate of glucose metabolism increased by 68%, from 56.2 (before rosiglitazone) to 94.2 (after rosiglitazone) mg/ (m^2-min) (p=0.002). During the high-dose clamps, the mean insulin-stimulated rate of glucose metabolism increased by 20%, from 296.0 (before rosiglitazone) to 356.0 mg/ m^2/min (after rosiglitazone) (p=0.016). The corresponding increases in the mean glucose disposal rate (GDR) were 119% during the low dose insulin clamps (34.8 ± 9.2 vs. 76.2 ± 9.9 mg/ (m^2-min), p=0.002) and 18% (340.2 ± 57.0 vs. 402.2 ± 37.1 mg/(m^2-min), p=0.10), during the high-dose insulin clamps. Rosiglitazone had no effect on basal glucose production (101.8 vs. 93.2 mg/ (m^2-min), p=0.12) or on the ability of insulin to suppress glucose production during the second step of hyperinsulinemic-euglycemic clamp that was maximally suppressed in both studies.

Glucose and Lipid Oxidation—Basal and insulin-stimulated rates of glucose and lipid oxidation were unchanged by rosiglitazone therapy (Table 2).

Whole body Glycerol Turnover—Whole-body glycerol turnover was similar before and after treatment at baseline (before: 7.6±1.2 vs after 7.6±1.0 mg/m^2-min, p = 0.99) and during both the low-dose (before 3.2 ± 0.7 vs. after 2.8 ± 0.5 mg/m^2-min, p = 0.34) and high-dose (before 2.6 ± 0.4 vs. after 3.0 ± 0.5 mg/m^2-min, p = 0.34) steps of the insulin clamp.

Microdialysis

Adipocyte Response to Insulin—Rosiglitazone therapy led to a 52% increase in the percent suppression of glycerol release from adipocytes by insulin during the low-dose insulin clamp (28.5±6.3 vs. 43.3±7.4%, p=0.04). There was no significant difference in baseline microdialysis glycerol concentration or percent suppression during the high-dose

insulin clamp (Figure 2). Relative changes in adipocyte blood flow were estimated by measuring the ratio of $ETOH_{out}$: $ETOH_{in}$, representing the concentration of ethanol in the dialysate versus that in the perfusate during the microdialysis procedure as previously described and validated (26,27). A lower ratio indicates decreased ETOH recovery and therefore an increase in local blood flow. There was no effect of rosiglitazone on the percent change in ETOH recovery during the low-dose clamp (before; 4.8 ± 2.3 vs. after; 5.0 ± 4.7, p= 0.96).

Tissue Lipid Content

Hepatic Lipid Content—Three months of rosiglitazone treatment caused a 39% decrease in hepatic triglyceride content (9.3 ± 2.5 vs. 5.7 ± 1.5%, p< 0.05) (Figure 3).

Muscle Lipid Content—Intramyocellular lipid content (IMCL) did not change significantly following rosiglitazone therapy (2.5 ± 0.4 vs. 2.7 ± 0.6%, p=0.50). In contrast extramyocellular lipid content (EMCL) increased by 39%, from 1.9 ± 0.50 to 2.7 ± 0.5%, p=0.03) following three months of rosiglitazone treatment (Figure 3).

Body Composition—There were no detectable changes in body weight or body composition as assessed by DEXA between baseline recordings and that at the conclusion of three months of rosiglitazone therapy; (body weight: 92.3 ± 3.0 vs. 93.9 ± 5.7 kg, p=0.34; lean body mass 61.3 ± 3.4 vs. 59.9 ± 2.5 kg, p= 0.98; percent body fat 29.9% ± 3.6% vs. 33.1% ± 4.5%, p=0.78).

Discussion

Three months of rosiglitazone treatment resulted in a significant improvement in insulin stimulated glucose disposal that could mostly be attributed to an increase in nonoxidative glucose metabolism. These results are similar to the results from previous hyperinsulinemic-euglycemic clamp studies examining troglitazone treatment in patients with type 2 diabetic subjects (3–5). This improvement in insulin responsiveness was associated with a marked reduction in hepatic triglyceride content and an increase in extramyocellular triglyceride content. Furthermore we found that rosiglitazone treatment resulted in a significant improvement in peripheral adipocyte insulin responsiveness as reflected by an increase in insulin suppression of peripheral adipocyte lipolysis and decreased plasma fatty acid concentrations. Overall these results are consistent with the hypothesis that thiazolidinediones improves insulin sensitivity in patients with type 2 diabetes by activating PPAR–γ receptors in peripheral adipocytes and promoting adipocyte differentiation (33,34). This results in an increase in smaller and more insulin responsive adipocytes which in turn leads to lower circulating plasma fatty acid concentrations and a redistribution of lipid (and intracellular fatty acid metabolites) from liver and muscle to peripheral adipocytes. Consistent with this theory are the recent findings that rosiglitazone's antidiabetic effect is severely curtailed in an insulin resistant transgenic mouse model of lipoatrophy (35).

The marked reduction that we observed in hepatic triglyceride content was associated with decreases in both serum alkaline phosphatase and γ–glutaryltranspeptidase (GGT), both markers of hepatic infiltration that are frequently elevated in steatohepatitis. These data suggest that TZD therapy may be useful in patients with non-alcoholic steatohepatitis (NASH), which has been associated with insulin resistance, obesity and diabetes. Specific studies of patients with more severe fatty infiltration may further clarify this tissue.

Surprisingly, we found that rosiglitazone caused no significant decrease in intramyocellular triglyceride content, despite a significant improvement in muscle insulin sensitivity. In contrast Ye et al. have recently reported that pioglitazone decreased triglyceride and fatty

acyl CoA content in skeletal muscle of Zucker rats (36). While species differences might explain these discrepant results it is more likely that intramuscular triglyceride content is just a marker for another intramyocellular fatty acid metabolite, such as fatty acyl CoA, that is actually responsible for events leading to decreased IRS-1 associated phopshoinositol 3-kinase activity (34).

In contrast rosiglitazone treatment caused a significant increase in extramyocellular lipid content, which is consistent with its effects to promote adipocyte differentiation and suggests that extramyocellular adipocytes behave similar to peripheral adipocytes in response to thiazolidinediones. These findings are consistent with the results of Kelley et al. who found that three months of troglitazone therapy in subjects with type 2 diabetes improved fasting plasma glucose concentrations while increasing total body fat mass (37). Body composition analysis by computer tomography revealed that this increase was exclusively attributable to an increase in peripheral adiposity, while visceral fat stores decreased. Similar results have been achieved by other groups, using troglitazone (38–41) and pioglitazone (42) in patients with type 2 diabetes and lipodystrophy (43). This "redistribution" of body fat may result from the predilection for certain PPAR–γ agonists to induce preadipocyte differentiation in subcutaneous rather than visceral fat depots (45).

It is also possible that rosiglitazone improves insulin sensitivity in type 2 diabetes by altering the concentrations of certain adipocyte derived hormones such as leptin (6), TNF–α, adiponectin (7), or resistin (9). In regards to leptin we found no significant effects of rosiglitazone on either fasting or insulin-stimulated leptin concentrations. Previous *in vitro* and *in vivo* studies on the effects of TZDs on leptin production by adipocytes have yielded conflicting results (45–49). Nolan et al. showed that coincubation of adipocytes with troglitazone abolished the usual two-fold increase in insulin-stimulated leptin production *in vitro* (45). In contrast rosiglitazone had no effect on plasma leptin concentrations in obese Zucker rats (46). In obese, non-diabetic human subjects, troglitazone caused no change in leptin levels but it has been shown to decrease leptin concentrations in diabetic subjects (47,48). Based on our results, alteration in circulating leptin concentrations does not appear to be playing a major role in mediating the insulin sensitizing effects of rosiglitazone. The effects of rosiglitazone on other circulating fat derived factors, such as resistin, TNF–α, adiponectin, which may modify insulin sensitivity in type 2 diabetic subjects remains to be determined.

In summary, we found that three months of rosiglitazone treatment resulted in an improvement in insulin responsiveness in type 2 diabetic subjects that was associated with a marked reduction in hepatic triglyceride content and an increase in extramyocellular lipid content. These changes were associated with an enhancement of insulin's ability to suppress peripheral adipocyte lipolysis. Overall these results support the hypothesis that thiozolodinediones enhance insulin sensitivity in patients with type 2 diabetes by promoting increased insulin sensitivity in peripheral adipocytes, which results in a redistribution of intracellular lipid from insulin responsive organs into adipocytes.

Acknowledgments

The authors which to thank Fran Rife and Yanna Kosover for their assistance with these studies. This work was supported by grants from the United States Public Health Service (R01 DK-49230, P30 DK-45735, M01 RR-00125 and a K-23 award (KFP)) and a grant from Glaxo Smith-Kline (to KFP).

References

1. Day C. Thiazolidinediones: a new class of antidiabetic drugs. Diabet Med 1999;16:179–192. [PubMed: 10227562]

2. Tontonoz P, Hu E, Spiegelman BM. Regulation of adipocyte gene expression and differentiation by peroxisome proliferator activated receptor gamma. Curr Opin Genet Devel 1995;5:571–576. [PubMed: 8664544]
3. Maggs DG, Buchanan TA, Burant CF, Cline G, Gumbiner B, Hsueh WA, Inzucchi S, Kelley D, Nolan J, Olefsky JM, Polonsky KS, Valiquett TR, Shulman GI. Metabolic effects of troglitazone monotherapy in type 2 diabetes mellitus: a randomized, double-blind, placebo-controlled trial. Ann Intern Med 1998;128:176–185. [PubMed: 9454525]
4. Inzucchi SE, Maggs DG, Spollett GR, Page SL, Rife FS, Walton V, Shulman GI. Efficacy and metabolic effects of metformin and troglitazone in type II diabetes mellitus. N Engl J Med 1998;338:867–872. [PubMed: 9516221]
5. Petersen KF, Krssak M, Inzucchi S, Cline GW, Dufour S, Shulman GI. Mechanism of troglitazone action in type 2 diabetes. Diabetes 2000;49:827–831. [PubMed: 10905493]
6. Shimomura H, Hammer RE, Ikemoto S, Brown MS, Goldstein JL. Leptin reverses insulin resistance and diabetes mellitus in mice with congenital lipodystrophy. Nature 1999;401:73–76. [PubMed: 10485707]
7. Yamauchi T, Kamon J, Waki H, Terauchi Y, Kubota N, Hara K, Mori Y, Ide T, Murakami K, Tsuboyama-Kasaoka N, Ezaki O, Akanuma Y, Gavrilova O, Vinson C, Reitman ML, Kagechika H, Shudo K, Yoda M, Nakano Y, Tobe K, Nagai R, Kimura S, Tomita M, Froguel P, Kadowaki T. The fat-derived hormone adiponectin reverses insulin resistance associated with both lipoatrophy and obesity. Nature Med 2001;7:941–946. [PubMed: 11479627]
8. Hotamisligil GS, Shargill NS, Spiegelman BM. Adipose expression of tumor necrosis factor-alpha: direct role in obesity-linked insulin resistance. Science 1993;259:87–91. [PubMed: 7678183]
9. Steppan CM, Bailey ST, Bhat S, Brown EJ, Banerjee RR, Wright CM, Patel HR, Ahima RS, Lazar MA. The hormone resistin links obesity to diabetes. Nature 2001;409:307–312. [PubMed: 11201732]
10. Boden G, Chen X. Effects of fat on glucose uptake and utilization in patients with non-insulin-dependent diabetes. J Clin Invest 1995;96:1261–1268. [PubMed: 7657800]
11. Roden M, Price TB, Perseghin G, Petersen KF, Rothman DL, Cline GW, Shulman GI. Mechanism of free fatty acid-induced insulin resistance in humans. J Clin Invest 1996;97:2859–2865. [PubMed: 8675698]
12. Dresner A, Laurent D, Marcucci M, Griffin ME, Dufour S, Cline GW, Slezak LA, Andersen DK, Hundal RS, Rothman DL, Petersen KF, Shulman GI. Effects of free fatty acids on glucose transport and IRS-1-associated phosphatidylinositol 3-kinase activity. J Clin Invest 1999;103:253–259. [PubMed: 9916137]
13. Griffin ME, Marcucci MJ, Cline GW, Bell K, Barucci N, Lee D, Goodyear LJ, Kraegen EW, White MF, Shulman GI. Free fatty acid-induced insulin resistance is associated with activation of protein kinase C theta and alterations in the insulin signaling cascade. Diabetes 1999;48:1270–1274. [PubMed: 10342815]
14. Perseghin G, Scifo P, De Cobelli F, Pagliato E, Battezzati A, Arcelloni C, Vanzulli A, Testolin G, Pozza G, Del Mascio A, Luzi L. Intramyocellular triglyceride content is a determinant of in vivo insulin resistance in humans. Diabetes 1999;48:1600–1606. [PubMed: 10426379]
15. Kim JK, Gavrilova O, Chen Y, Reitman ML, Shulman GI. Mechanism of insulin resistance in A-ZIP/F-1 fatless mice. J Biol Chem 2000;275:8456–8460. [PubMed: 10722680]
16. Kim JK, Fillmore JJ, Chen Y, Yu C, Moore IK, Pypaert M, Lutz EP, Kako Y, Velez-Carrasco W, Goldberg IJ, Breslow JL, Shulman GI. Tissue-specific overexpression of lipoprotein lipase causes tissue-specific insulin resistance. Proc Nat Acad Sci USA 2001;98:7522–7527. [PubMed: 11390966]
17. Krssak M, Falk Petersen K, Dresner A, DiPietro L, Vogel SM, Rothman DL, Roden M, Shulman GI. Intramyocellular lipid concentrations are correlated with insulin sensitivity in humans: a ^{1}H NMR spectroscopy study. Diabetologia 1999;42:113–116. [PubMed: 10027589]
18. Pan DA, Lillioja S, Kriketos AD, Milner MR, Baur LA, Bogardus C, Jenkins AB, Storlien LH. Skeletal muscle triglyceride levels are inversely related to insulin action. Diabetes 1997;46:983–988. [PubMed: 9166669]

19. Jucker BM, Cline GW, Barucci N, Shulman GI. Differential effects of safflower oil versus fish oil feeding on insulin-stimulated glycogen synthesis, glycolysis, and pyruvate dehydrogenase flux in skeletal muscle: a 13C nuclear magnetic resonance study. Diabetes 1999;48:134–140. [PubMed: 9892234]
20. Laybutt DR, Schmitz-Peiffer C, Saha AK, Ruderman NB, Biden TJ, Kraegen EW. Muscle lipid accumulation and protein kinase C activation in the insulin-resistant chronically glucose-infused rat. Am J Physiol 1999;277(6 Pt 1):E1070–E1076. [PubMed: 10600797]
21. Ryysy L, Hakkinen AM, Goto T, Vehkavaara S, Westerbacka J, Halavaara J, Yki-Jarvinen H. Hepatic fat content and insulin action on free fatty acids and glucose metabolism rather than insulin absorption are associated with insulin requirements during insulin therapy in type 2 diabetic patients. Diabetes 2000;49:749–758. [PubMed: 10905483]
22. Lusk G. Animal calorimetry:analysis of the oxidation of mixtures of carbohydrates and fat: a correction. J Biol Chem 1924;59:41–42.
23. Lafontan M, Arner P. Application of *in situ* microdialysis to measure metabolic and vascular responses in adipose tissue. TIPS 1996;17:309–313. [PubMed: 8885693]
24. Tossman U, Ungerstedt U. Microdialysis in the study of extracellular levels of amino acids in the rat brain. Acta Physiol Scand 1986;128:9–14. [PubMed: 2876587]
25. Arner P, Bulow J. Assessment of adipose tissue metabolism in man-comparison of Fick and microdialysis techniques. Clin Sci 1993;82:247–256. [PubMed: 8403794]
26. Hickner RC, Rosdahl H, Borg I, Ungerstedt U, Jorfeldt L, Henricksson J. Ethanol may be used with the microdialysis technique to monitor blood flow changes in skeletal muscle:dialysate glucose concentrations is bloodflow dependent. Acta Physiol Scand 1992;146:87–97. [PubMed: 1442130]
27. Fellander G, Linde B, Bolinder J. Evaluation of the microdialysis ethanol technique for monitoring of subcutaneous adipose tissue blood flow in humans. Int JObesity 1996;20:220–226.
28. Shen J, Rycyna RE, Rothman DL. Improvements on an *in vivo* automatic shimming method [FASTERMAP]. Mag Reson Med 1997;38:834–839.
29. Schick F, Eismann B, Jung WI, Bongers H, Bunse M, Lutz O. Comparison of localized proton NMR signals of skeletal muscle and fat tissue in vivo: two lipid compartments in muscle tissue. Mag Reson Med 1993;29:158–167.
30. Brozek JF, Grande JT, Andersen T, Keys A. Densitometric analysis of body composition: revision of some quantitative assumptions. Ann NY Acad Sci 1963;110:113–140. [PubMed: 14062375]
31. Miles J, Glasscock R, Aikens J, Gerich J, Haymond M. A microfluorometric method for the determination of free fatty acids in plasma. J Lipid Res 1983;24:96–99. [PubMed: 6833886]
32. Wolfe, RR. Radioactive and Stable Isotope Tracers in Biomedicine: Principles and Practice of Kinetic Analysis. New York: Wiley-Liss; 1992.
33. Okuno A, Tamemoto H, Tobe K, Ueki K, Mori Y, Iwamoto K, Umesono K, Akanuma Y, Fujiwara T, Horikoshi H, Yazaki Y, Kadowaki T. Troglitazone increases the number of small adipocytes without the change of white adipose tissue mass in obese Zucker rats. J Clin Invest 1998;101:1354–1361. [PubMed: 9502777]
34. Shulman GI. Cellular mechanisms of insulin resistance. J Clin Invest 2000;106:171–176. [PubMed: 10903330]
35. Chao L, Marcus-Samuels B, Mason MM, Moitra J, Vinson C, Arioglu E, Gavrilova O, Reitman ML. Adipose tissue is required for the antidiabetic, but not for the hypolipidemic, effect of thiazolidinediones. J Clin Invest 2000;106:1221–1228. [PubMed: 11086023]
36. Ye JM, Doyle PJ, Iglesias MA, Watson DG, Cooney GJ, Kraegen EW. Peroxisome proliferator-activated receptor (PPAR)-alpha activation lowers muscle lipids and improves insulin sensitivity in high fat-fed rats: comparison with PPAR-gamma activation. Diabetes 2001;50:411–417. [PubMed: 11272155]
37. Kelly IE, Han TS, Walsh K, Lean ME. Effects of a thiazolidinedione compound on body fat and fat distribution of patients with type 2 diabetes. Diabetes Care 1999;22:288–293. [PubMed: 10333947]

38. Mori Y, Murakawa Y, Okada K, Horikoshi H, Yokoyama J, Tajima N, Ikeda Y. Effect of troglitazone on body fat distribution in type 2 diabetic patients. Diabetes Care 1999;22:908–912. [PubMed: 10372240]
39. Kawai T, Takei I, Oguma Y, Ohashi N, Tokui M, Oguchi S, Katsukawa F, Hirose H, Shimada A, Watanabe K, Saruta T. Effects of troglitazone on fat distribution in the treatment of male type 2 diabetes. Metab Clin Exp 1999;48:1102–1107. [PubMed: 10484048]
40. Akazawa S, Sun F, Ito M, Kawasaki E, Eguchi K. Efficacy of troglitazone on body fat distribution in type 2 diabetes. Diabetes Care 2000;23:1067–1071. [PubMed: 10937499]
41. Katoh S, Hata S, Matsushima M, Ikemoto S, Inoue Y, Yokoyama J, Tajima N. Troglitazone prevents the rise in visceral adiposity and improves fatty liver associated with sulfonylurea therapy - a randomized controlled trial. Metab Clin Exp 2001;50:414–417. [PubMed: 11288035]
42. Miyazaki Y, Mahankali A, Matsuda M, Mahankali S, Cusi K, Mandarino J, Defronzo RA. Relationship between visceral fat and inhanced peripheral/hepatic insulin sensitivity after pioglitazone in type 2 diabetes. Diabetes 2001;50 Suppl 2:A126.
43. Arioglu E, Duncan-Morin J, Sebring N, Rother KI, Gottlieb N, Lieberman J, Herion D, Kleiner DE, Reynolds J, Premkumar A, Sumner AE, Hoofnagle J, Reitman ML, Taylor SI. Efficacy and safety of troglitazone in the treatment of lipodystrophy syndromes. Ann Intern Med 2000;133:263–274. [PubMed: 10929166]
44. Adams M, Montague CT, Prins JB, Holder JC, Smith SA, Sanders L, Digby JE, Sewter CP, Lazar MA, Chatterjee VK, O'Rahilly S. Activators of peroxisome proliferator-activated receptor gamma have depot-specific effects on human preadipocyte differentiation. J Clin Invest 1997;100:3149–3153. [PubMed: 9399962]
45. Nolan JJ, Olefsky JM, Nyce MR, Considine RV, Caro JF. Effect of troglitazone on leptin production: studies *in vitro* and in human subjects. Diabetes 1996;45:1276–1278. [PubMed: 8772734]
46. Wang Q, Dryden S, Frankish HM, Bing C, Pickavance L, Hopkins D, Buckingham R, Williams G. Increased feeding in fatty Zucker rats by the thiazolidinedione BRL 49653 (rosiglitazone) and the possible involvement of leptin and hypothalamic neuropeptide Y. Brit J Pharmacol 1997;122:1405–1410. [PubMed: 9421288]
47. Shimizu H, Tsuchiya T, Sato N, Shimomura Y, Kobayashi I, Mori M. Troglitazone reduces leptin concentration but increases hunger in NIDDM patients. Diabetes Care 1998;21:1470–1474. [PubMed: 9727893]
48. Mantzoros CS, Dunaif A, Flier JS. Leptin concentrations in the polycystic ovary syndrome. J Clin Endocrinol Metab 1997;82:1687–1691. [PubMed: 9177364]

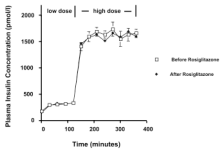

Figure 1.
Plasma insulin concentrations during the two step hyperinsulinemic-euglycemic clamp before and after rosiglitazone.

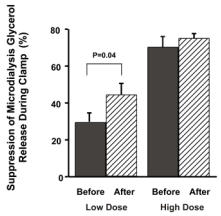

Figure 2.
Effects of three months of rosiglitazone treatment on insulin suppression of peripheral adipocyte lipolysis during the two-step hyperinsulinemic-euglycemic clamp.

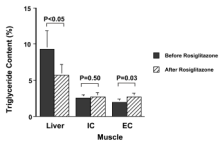

Figure 3.
Effects of three months of rosiglitazone treatment on hepatic triglyceride, intramyocellular triglyceride (IMCL) and extramyocellular triglyceride (EMCL) content.

TABLE 1

Baseline Characteristics of Study Subjects (n=9)

Age (years)	52 ± 3
Male/Female	5/4
Weight (kg)	92.3 ± 6.2
BMI (kg/m^2)	31.1 ± 1.6
Percent body fat (% fat mass/body mass)	29.9 ± 3.6
BSA (m^2)	2.04 ± 0.08
Baseline laboratory values	
HbA1c (%)	6.7
Fasting Glucose (mM)	9.1 ± 0.9
Fasting Insulin (pmol/L)	93.6 ± 13.8
Fasting C-peptide (pmol/L)	0.83 ± 0.0.08
Total Cholesterol (mM)	4.97 ± 0.39
HDL Cholesterol (mM)	0.88 ± 0.05
LDL Cholesterol (mM)	2.92 ± 0.34
Triglycerides (mM)	6.31 ± 1.66

TABLE 2

Basal fasting biochemical data before and after rosiglitazone therapy.

	Pre-rosiglitazone	**Post-rosiglitazone**	***p***
HbA1c (%)	6.7 ± 0.4%	7.2 ± 0.6%	0.23
Plasma Glucose (mM)	9.0 ± 0.9	7.9 ± 0.9	0.02
Insulin (pmol/L)	93.6 ± 13.8	71.4 ± 7.8	0.03
C-peptide (pmol/L)	0.83 ± 0.08	0.76 ± 0.06	0.19
Glucagon (ng/L)	87.0 ± 9.0	83.2 ± 7.3	0.54
Total Cholesterol (mM)	4.97 ± 0.39	5.43 ± 0.41	0.09
HDL Cholesterol (mM)	0.88 ± 0.05	0.96 ± 0.05	0.15
LDL Cholesterol (mM)	2.92 ± 0.34	3.31 ± 0.21	0.14
Triglycerides (mM)	6.31 ± 1.66	6.26 ± 1.34	0.97
Fatty acids (μmol/L)	497 ± 64	352 ± 55	0.003
Leptin (ng/ml)	21.1 ± 5.7	18.4 ± 4.7	0.34
Alkaline phosphatase(U/L)	72 ± 7	61 ± 7	0.007
γ–glutaryl transpeptidase (U/L)	29 ± 6	17 ± 3	0.001

TABLE 3

Rates of glucose and lipid oxidation before and after rosiglitazone therapy (mg/m^2-min).

	Pre-rosiglitazone	Post-rosiglitazone	p
Glucose oxidation			
Basal	32.4 ± 2.3	38.0 ± 5.0	0.24
Low-dose clamp	38.0 ± 2.9	46.6 ± 3.2	0.11
High-dose clamp	71.6 ± 4.7	73.5 ± 3.6	0.68
Lipid Oxidation			
Basal	158.5 ± 8.8	149.7 ± 17.3	0.24
Low-dose clamp	138.9 ± 12.4	122.1 ± 8.9	0.33
High-dose clamp	67.7 ± 13.7	71.1 ± 13.1	0.59